EO for Africa Symposium 2024

23 - 26 September 2024
ESA | ESRIN, Frascati (IT)

SpatioTemporal Dynamic Mapping of Landslide Susceptibility Based on Deep Learning and PS-InSAR coupling model

26/09/2024

TEAM REPRESENTATIVE

Kemche Ghomsi Adrien Arnaud, **Mvogo Ngono Joseph, Bowong Tsakou Samuel, Noumsi Woguia Auguste Vigny**
UNIVERSITY OF DOUALA, Cameroon
adrien.ghomsi@weloobe.com

SCIENTIFIC CONTEXT: Earth a chaotic systems

landslides are chaotic systems that can lead to signicant impacts

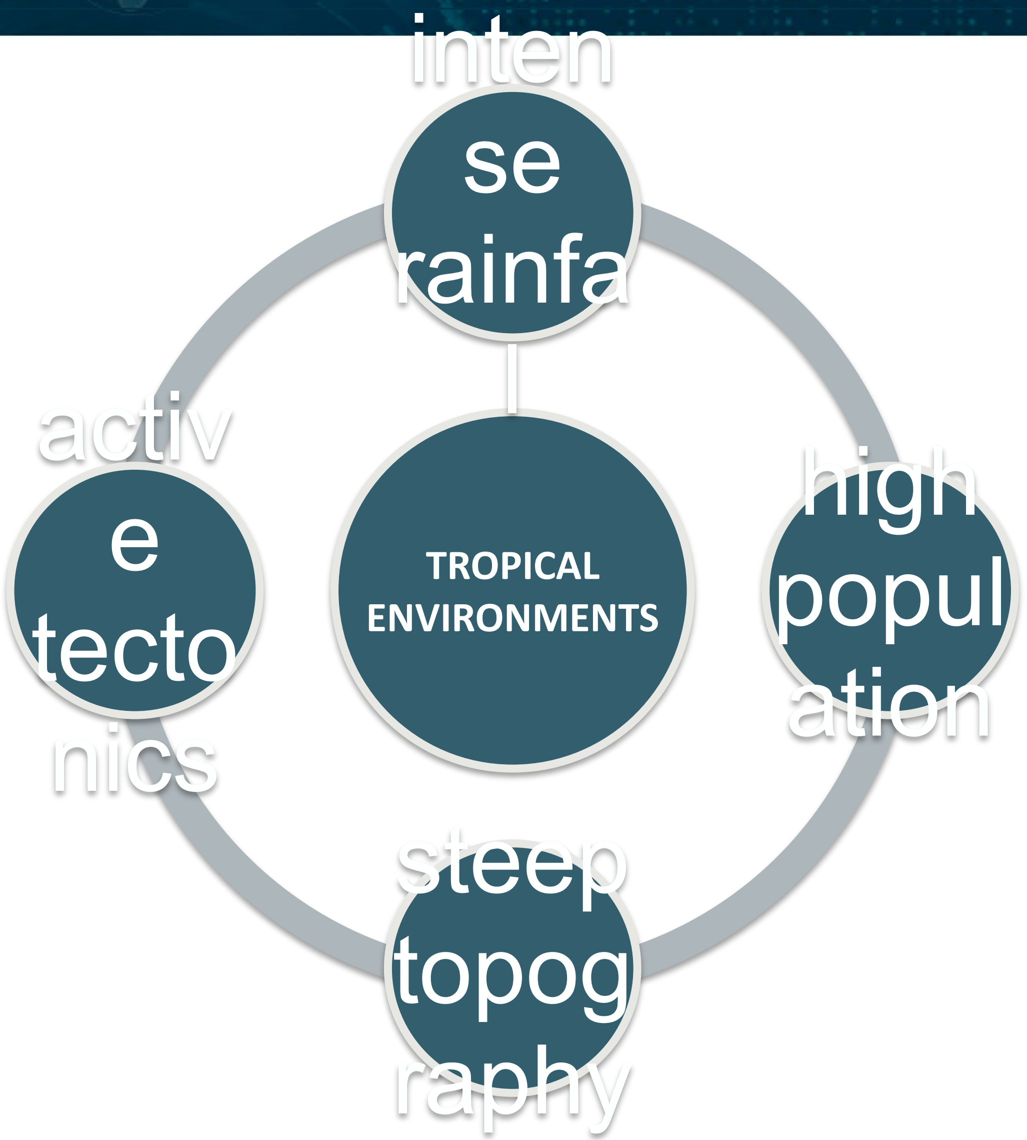

LANDISLDES are expected to increase due to population growth and climate change

Landslides can be triggered by various factors

Kirschbaum, D., Stanley, T.: Satellite-based assessment of rainfall-triggered landslide hazard for situational awareness. Earth's Future 6 (3), 505_x0015_523 (2018)

Xie, M., Esaki, T., Zhou, G., Mitani, Y.: Geographic information systems-based three-dimensional critical slope stability analysis and landslide hazard assessment. Journal of Geotechnical and Geoenvironmental engineering 129 (12), 1109_x0015_1118 (2003)

DeFries, R.S., Rudel, T., Uriarte, M., Hansen, M.: Deforestation driven by urban population growth and agricultural trade in the twenty-_x001C_rst century. Nature Geoscience 3 (3), 178_x0015_181 (2010)

Maes, J., Kervyn, M., de Hontheim, A., Dewitte, O., Jacobs, L., Mertens, K.,Vanmaercke, M., Vranken, L., Poesen, J.: Landslide risk reduction measures: A review of practices and challenges for the tropics. Progress in Physical Geography 41 (2), 191_x0015_221 (2017)

Knapen, A., Kitutu, M.G., Poesen, J., Breugelmans, W., Deckers, J., Muwanga, A.: Landslides in a densely populated county at the footslopes of mount elgon (uganda): characteristics and causal factors. Geomorphology 73 (1-2), 149_x0015_165 (2006)

initiation and their evolution

how to couple the spatio-temporal transformer with contextual trigger factors and the most powerful A-DinSAR technique, PS-inSAR, to predict a signature in dynamic landslide susceptibility mapping (LDSM) using Sentinel-1 data?

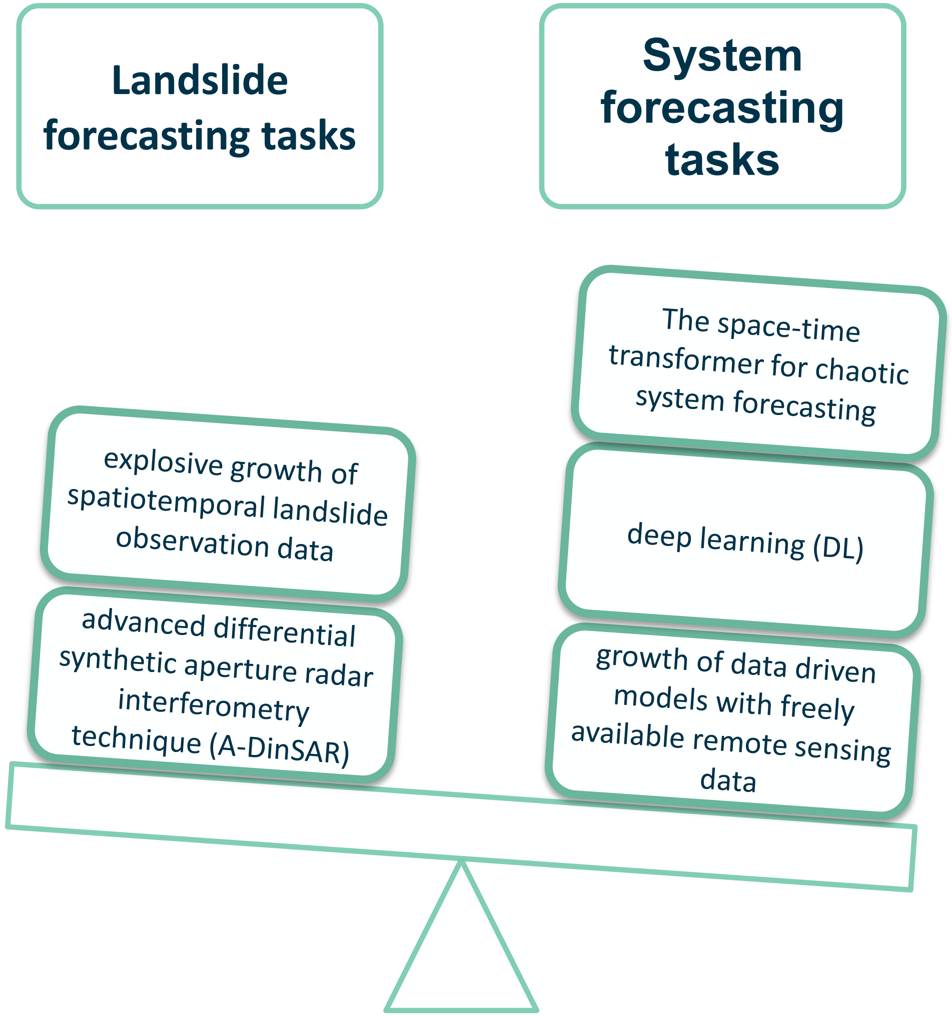

CONTEXTUAL TRIGGERS FACTOR
space-time input data: First Component

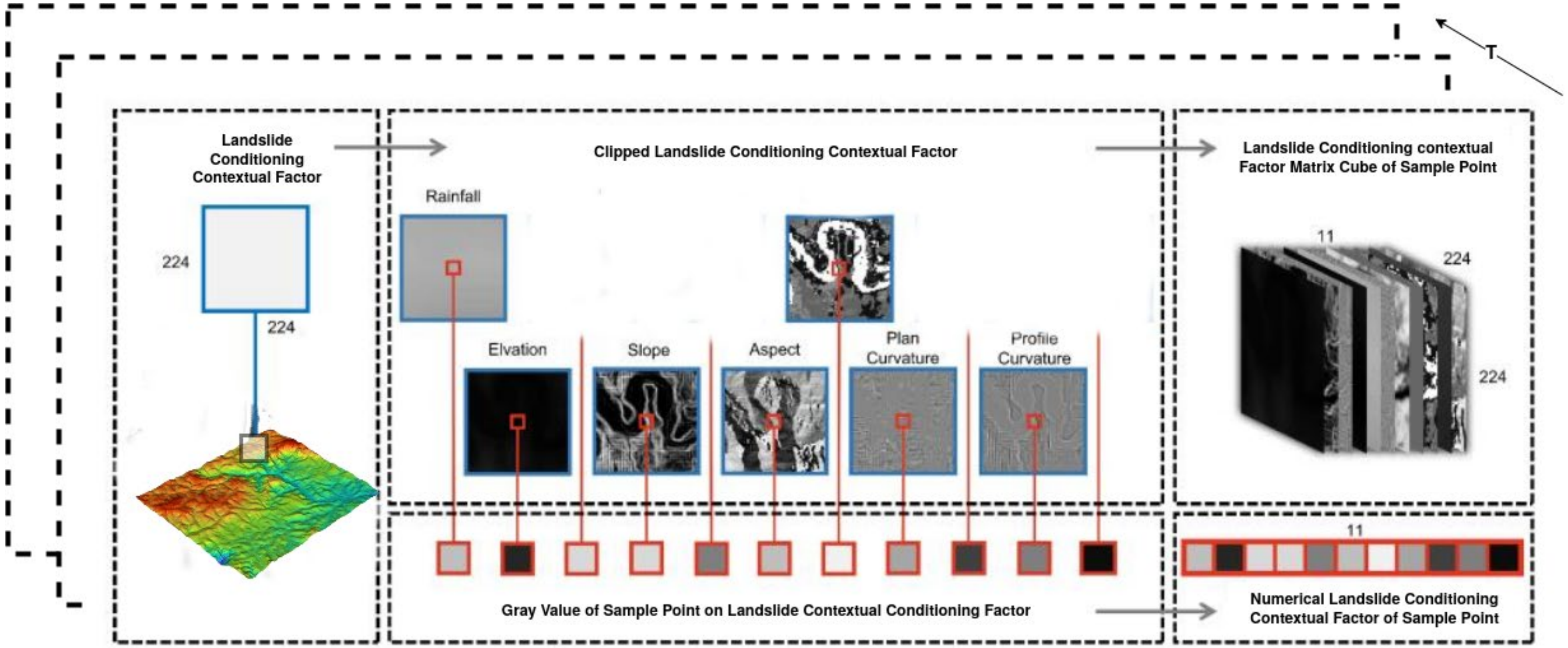

The first component, **contextual factors(07)**, includes a range of temporally related landslide data, encompassing parameters such as **"Elevation", "Slope", "Aspect", "Plan Curvature", "Profile Curvature", "Rainfall" and "Topographic Wetness Index" (TWI)**. This dataset is collected on a 12 and 24-daily basis, with each observation captured in a 1008x969 pixel frame

Barnes, R. (2018). RichDEM: High-performance terrain analysis (No. 27099v1). PeerJ Preprints.

FLOW CHART OF THE PROPOSED METHOD

1- Multi-Temporal CONTEXTUAL FACTORS EXTRACTION

2- Multi-Temporal MULTICOLLINEARITY ANALYSIS

3- Space-time UNSUPERVISED LEARNING

4- Natural Breakpoint Method and SUPERVISED CLASSIFICATION

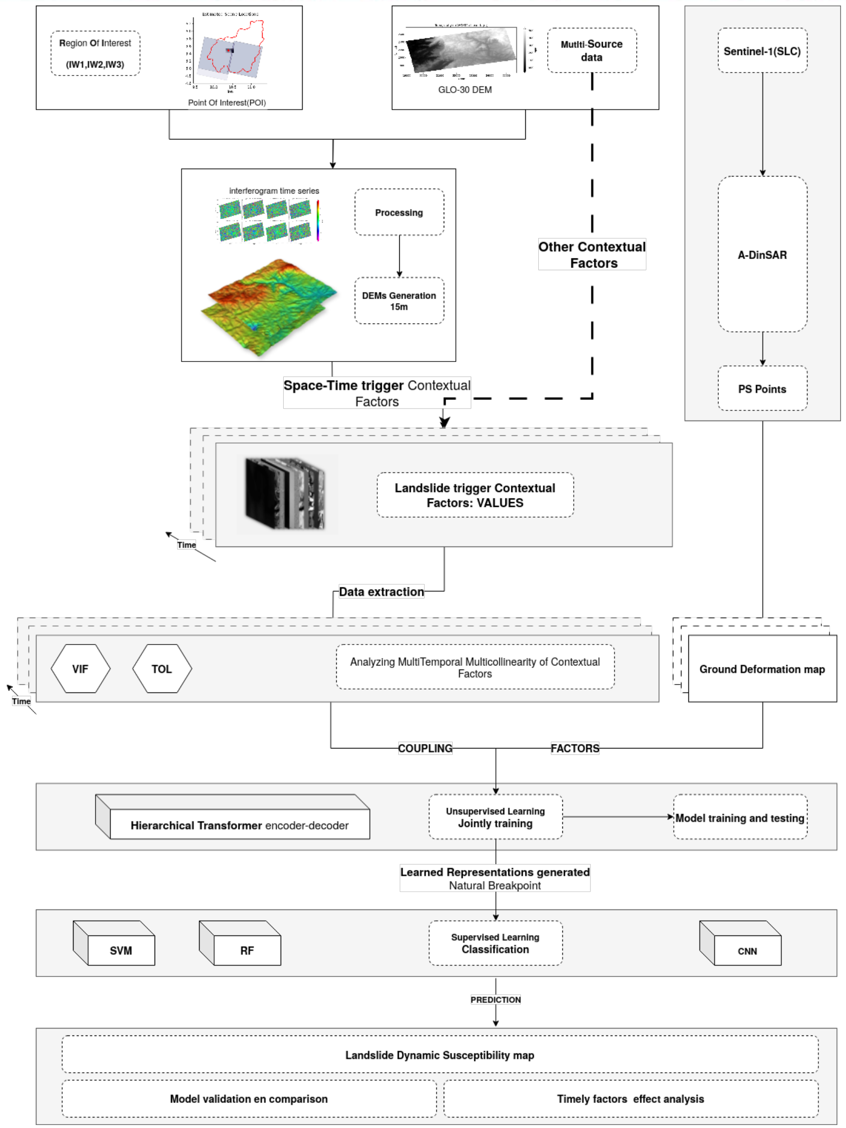

Baseline selection, generation of multi-temporal DEMs and extraction of contextual triggers factors

Braun, A.: Retrieval of digital elevation models from sentinel-1 radar data-open applications, techniques, and limitations. Open Geosciences 13 (1), 532-569 (2021)

Zevenbergen, L.W., Thorne, C.R.: Quantitative analysis of land surface topography. Earth surface processes and landforms 12 (1), 47-56 (1987)

Horn, B.K.: Hill shading and the reflectance map. Proceedings of the IEEE 69 (1), 14-47 (1981)

MITIGATE the impact of MT-Contextual Factors LINEAR CORRELATION

Liu, L.L., Yang, C., Huang, F.M., Wang, X.M.: Landslide susceptibility mapping by attentional factorization machines considering feature interactions. Geomatics, Natural Hazards and Risk 12 (1), 1837-1861 (2021)

transformers have shown to be very effective in capturing complex patterns and dependencies in sequential data

Gao, Z., Shi, X., Wang, H., Zhu, Y., Wang, Y.B., Li, M., Yeung, D.Y.: Earthformer: Exploring space-time transformers for earth system forecasting. Advances in Neural Information Processing Systems 35 , 25390-25403 (2022)

Classification of rich and contextual learned representations

Chen, L., Wang, W., Wu, W.B.: Inference of breakpoints in high-dimensional time series. Journal of the American Statistical Association 117 (540), 1951-1963 (2022)

STUDY AREA

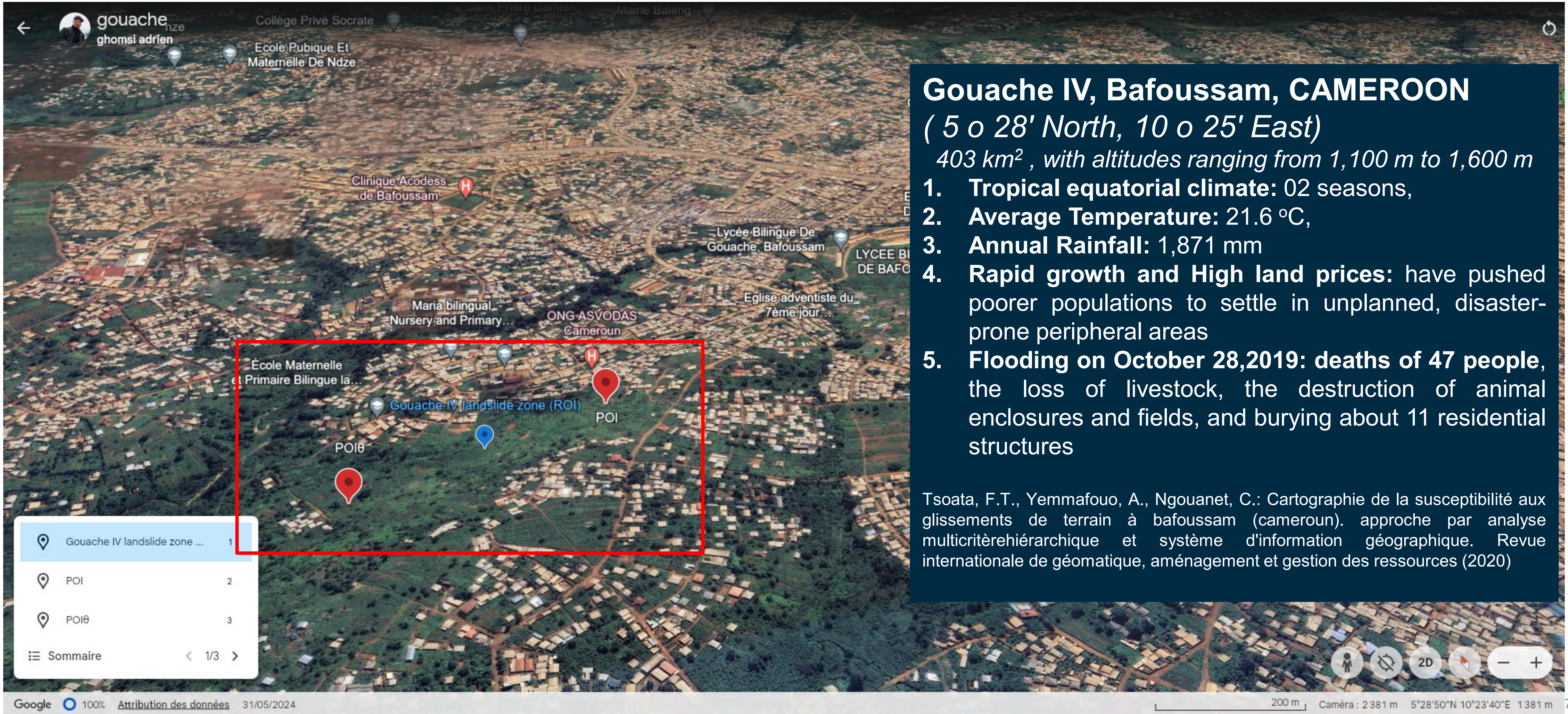

Gouache IV, Bafoussam, CAMEROON

(5 o 28' North, 10 o 25' East)

403 km^2 , with altitudes ranging from 1,100 m to 1,600 m

1. **Tropical equatorial climate:** 02 seasons,
2. **Average Temperature:** 21.6 °C,
3. **Annual Rainfall:** 1,871 mm
4. **Rapid growth and High land prices:** have pushed poorer populations to settle in unplanned, disaster-prone peripheral areas
5. **Flooding on October 28,2019: deaths of 47 people**, the loss of livestock, the destruction of animal enclosures and fields, and burying about 11 residential structures

Tsoata, F.T., Yemmafouo, A., Ngouanet, C.: Cartographie de la susceptibilité aux glissements de terrain à bafoussam (cameroun). approche par analyse multicritèrehiérarchique et système d'information géographique. Revue internationale de géomatique, aménagement et gestion des ressources (2020)

DATASET: Trend Baseline on our Study area(58 pairs in our dataset)

SHORT TEMPORAL BASELINE(58 PAIRS)

INITIAL DATASET of interferogram pairs with temporal baseline values less than a threshold of **24 days** for maintaining dataset consistency.(temporal baseline ranging from 12 to 24 days)

Braun, A.: Dem generation with sentinel-1 workflow and challenges. SkyWatch Space Applications Inc.: Waterloo, ON, Canada (2020)

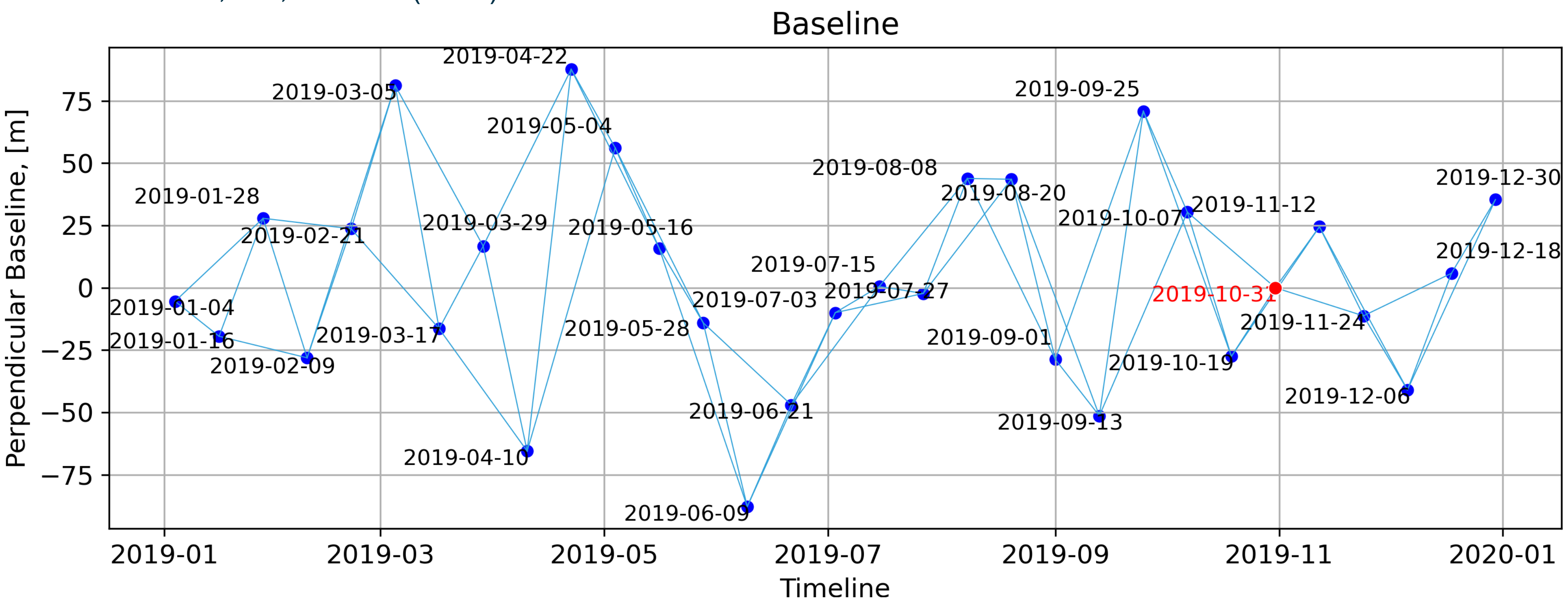

MultiTemporal - DEM GENERATION: on best pairs(24 pairs)

PERPENDICULAR BASELINE > 50m and < 300 m (24 PAIRS)

Our DATASET with 24 best pairs ensuring that the coherent phase did not become increasingly dissimilar is characterized by:

- temporal baseline ranging from **12 to 24 days**
- perpendicular baselines from **54.08 to 151.18 m**
- average coherence ranging from **0.27 to 0.34**

Braun, A.: Dem generation with sentinel-1 workflow and challenges. SkyWatch Space Applications Inc.: Waterloo, ON, Canada (2020)

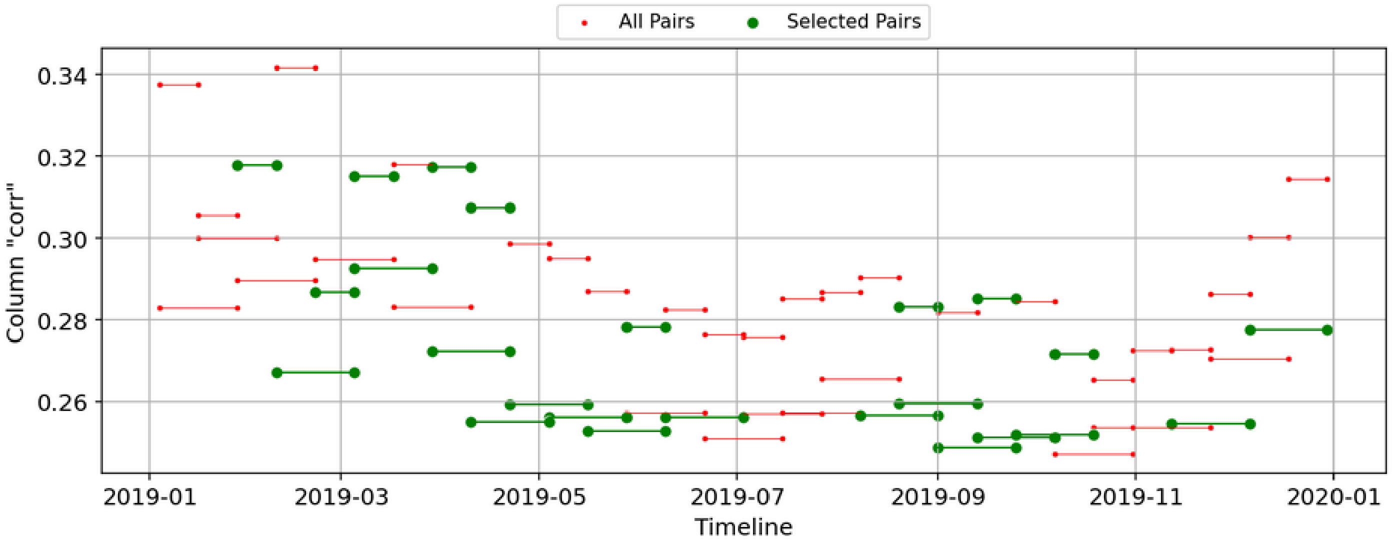

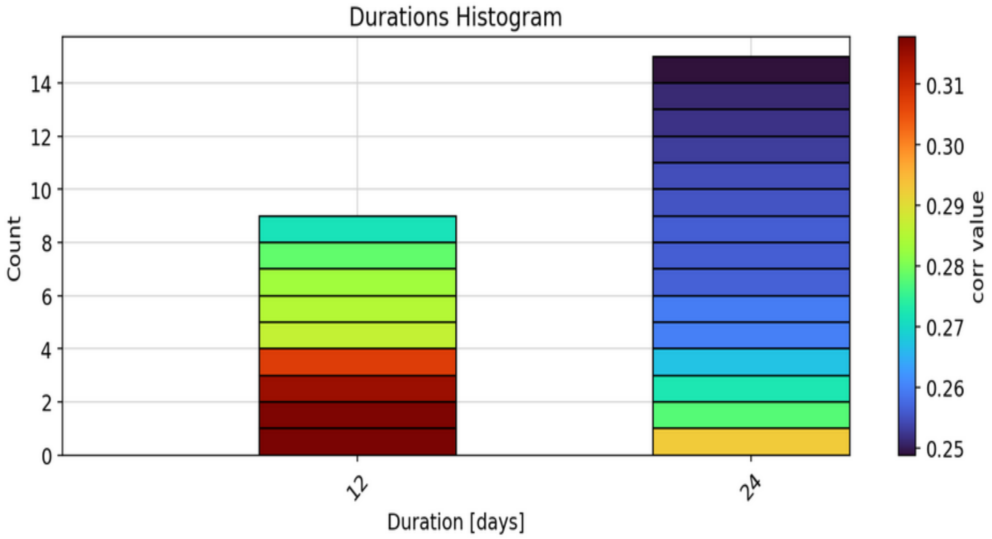

MultiTemporal - CONTEXTUAL TRIGGERS FACTORS EXTRACTION on best pairs(24 pairs)

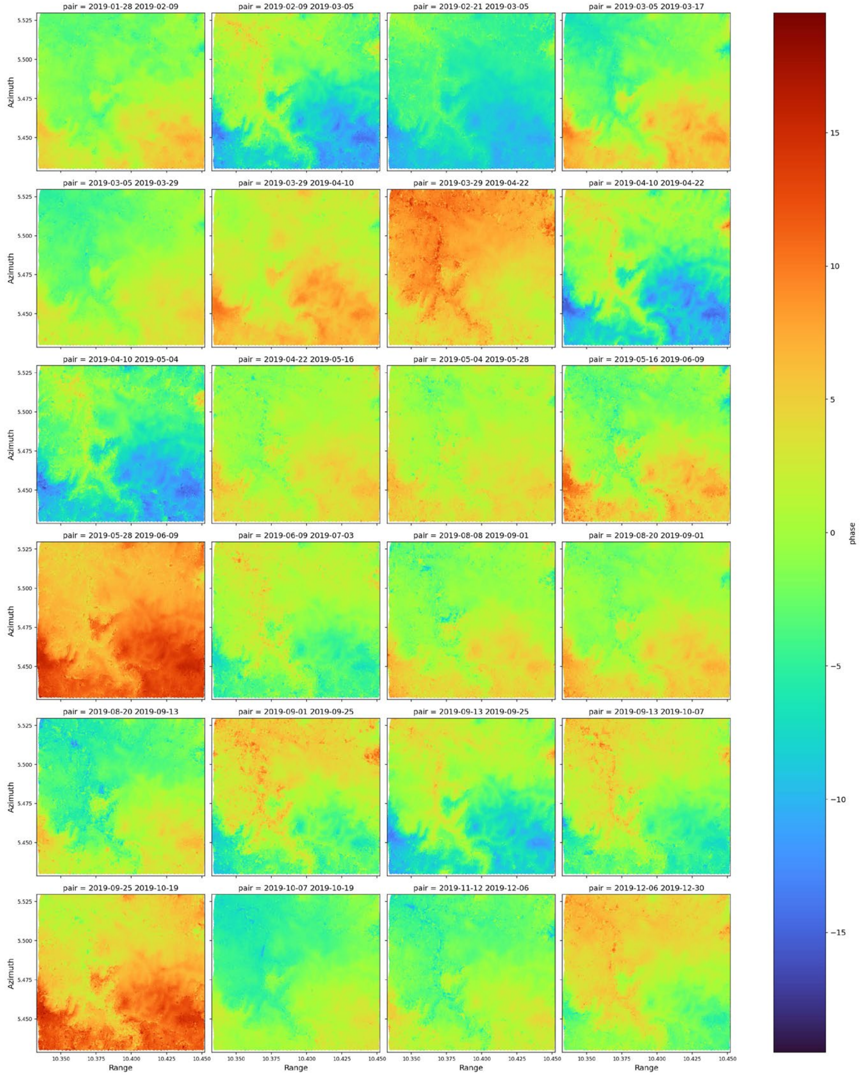

Unwrapped Phase in Geographic Coordinates

MultiTemporal -Triggers Factors extraction - techniques	
Elevation	Braun, A.: Dem generation with sentinel-1 workflow and challenges. SkyWatch Space Applications Inc.: Waterloo, ON, Canada (2020)
Slope	Horn, B.K.: Hill shading and the reflectance map. Proceedings of the IEEE 69 (1), 14-47 (1981)
Aspect	
Plan Curvature	Zevenbergen, L.W., Thorne, C.R.: Quantitative analysis of land surface topography. Earth surface processes and landforms 12 (1), 47-56 (1987)
Profil Curvature	
Rainfall(Millimeter)	Ebodé, V.B.: Analysis of the spatio-temporal rainfall variability in cameroon over the period 1950 to 2019. Atmosphere 13 (11), 1769 (2022)
TWI	Schmidt, F., Persson, A.: Comparison of dem data capture and topographic wetness indices. Precision Agriculture 4 , 179-92 (2003)

Triggers Factors	VIF	TOL
Elevation	0.920	1.087
Slope	0.958	1.044
Aspect	0.704	1.420
Plan Curvature	**1.707**	**0.586**
Profil Curvature	1.705	0.586
Rainfall(Millimeter)	**0.558**	**1.792**
TWI	0.989	1.011

VIF = Variance In_x001D_ation Factor
TOL = Tolerance

Seven triggers Factors:

- "Plan Curvature" and "Profile Curvature" factors show slightly higher VIF values In addition, their low TOL indicates that they have some redundancy, but not to the point of compromising the analyses
- Other variables, such as elevation , slope , aspect and Topographic Wetness Index, also show low VIF values, suggesting good independence.
- The variable Rainfall has the lowest VIF (0.557) and a high TOL (1.792), indicating that it is the least correlated with the other factors

The **VIF** values for **all factors are < 5, well below the critical threshold** indicating worrying MT-multicollinearity**.**

MultiTemproal - CONTEXTUAL TRIGGERS FACTORS NORMALISATION on best pairs(24 pairs)

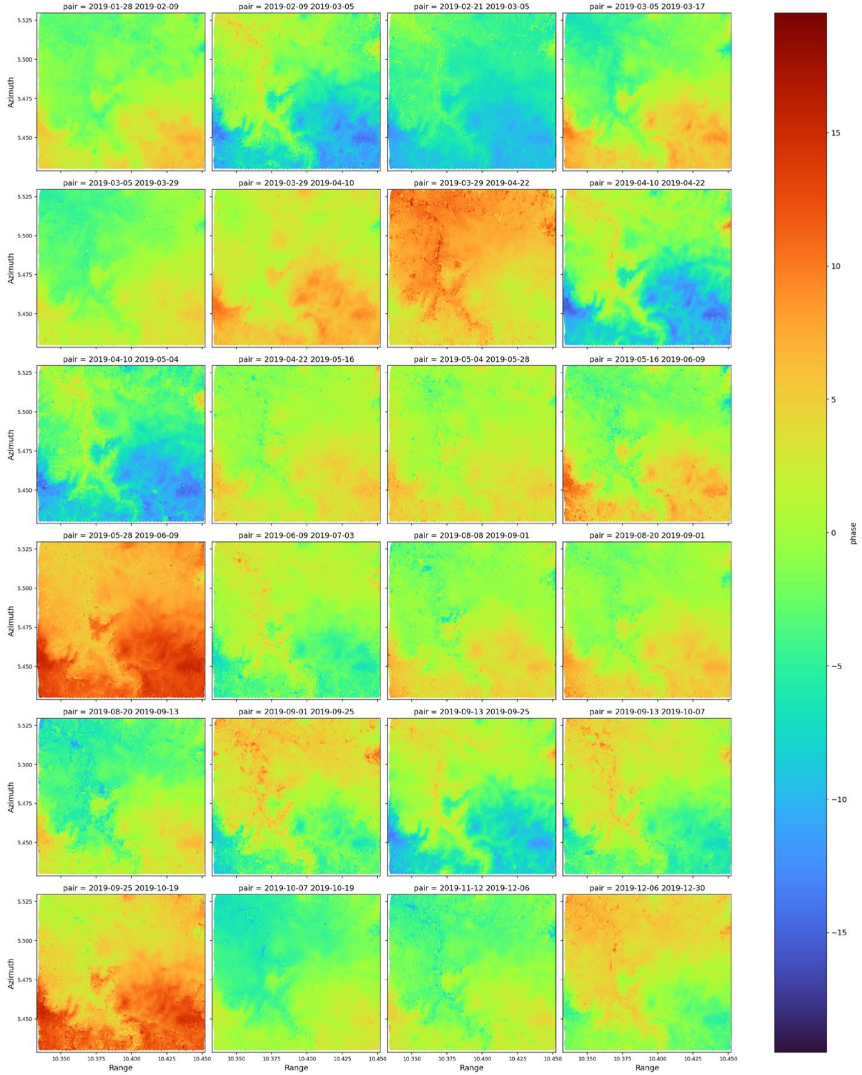

Unwrapped Phase in Geographic Coordinates

Triggers Factors
Elevation
Slope
Aspect
Plan Curvature
Profil Curvature
Rainfall(Millimeter)
TWI

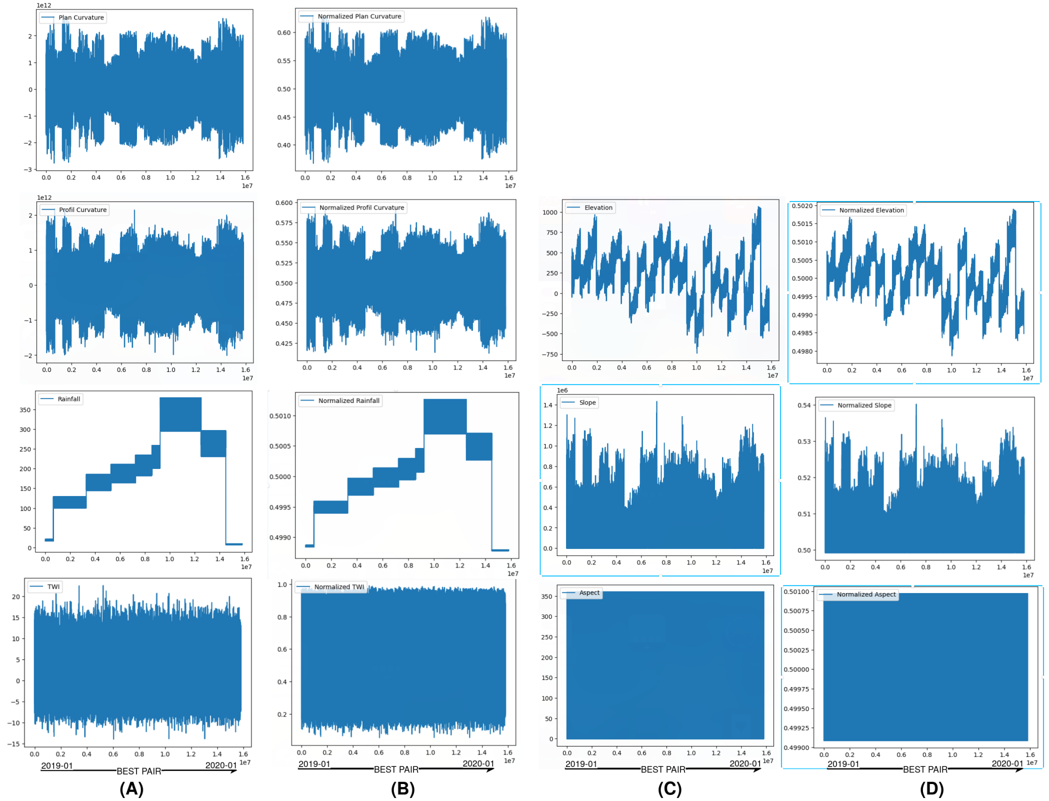

Triggers factors dataset on our selected region of interest, derived from DEMs generated **from January 2019 to January 2020**. (A) and (C) illustrate the dynamics of value variations over this period, while (B) and (D) represent data normalized to prepare the data for deep learning training. The high 12 variability of values ranges from 0 to around ±3 ∗ 10 and from 0 to 1 for normalized data

STACK CORRELATION
of the Best 24 Image

The **best pairs demonstrate a higher correlation** according to the correlation stack, **which represents the mean correlation value for each pixel in the correlation map of each optimal pair with a threshold greater than 0.100, along with a histogram median correlation value of 0.217.** This suggests an increased reliability in measuring surface deformations. This level of correlation is essential to minimize uncertainty in the results obtained and to ensure the validity of the analyses derived from the dataset.

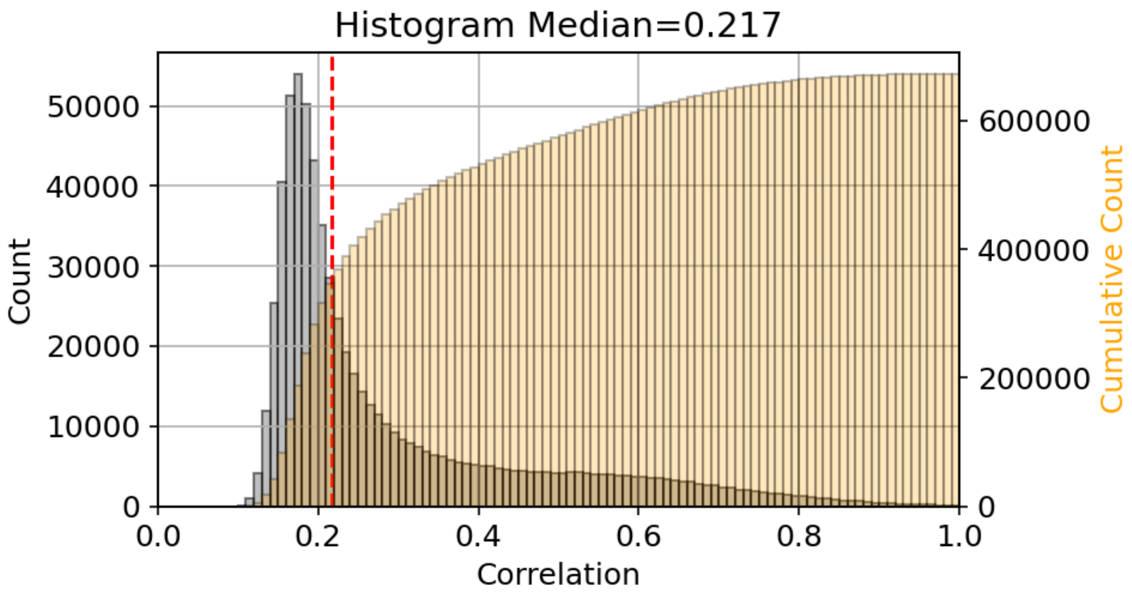

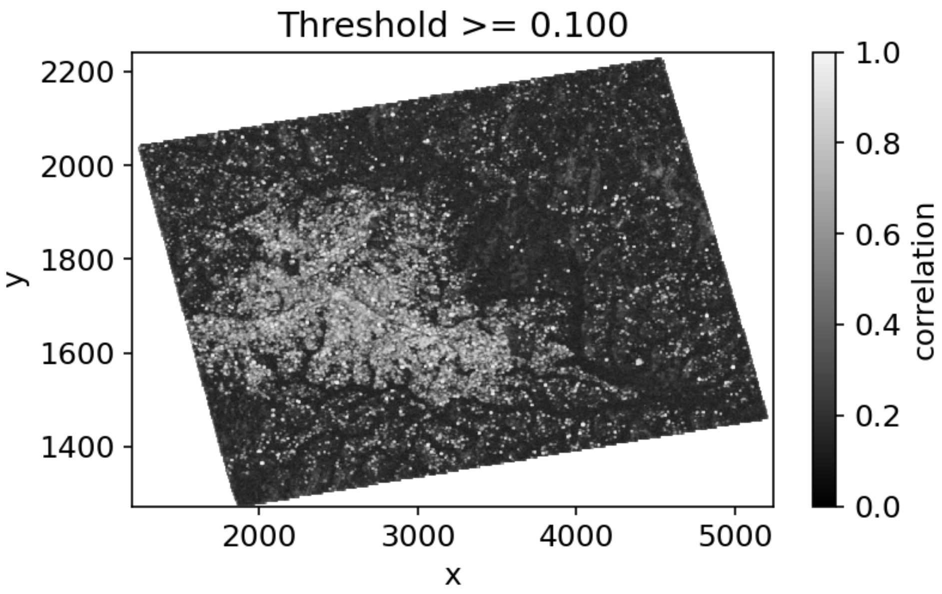

GROUND DYNAMIC(PS-INSAR)
space-time input data: Second Component

Ground Dynamic measurement
Phase
Coherence
Amplitude

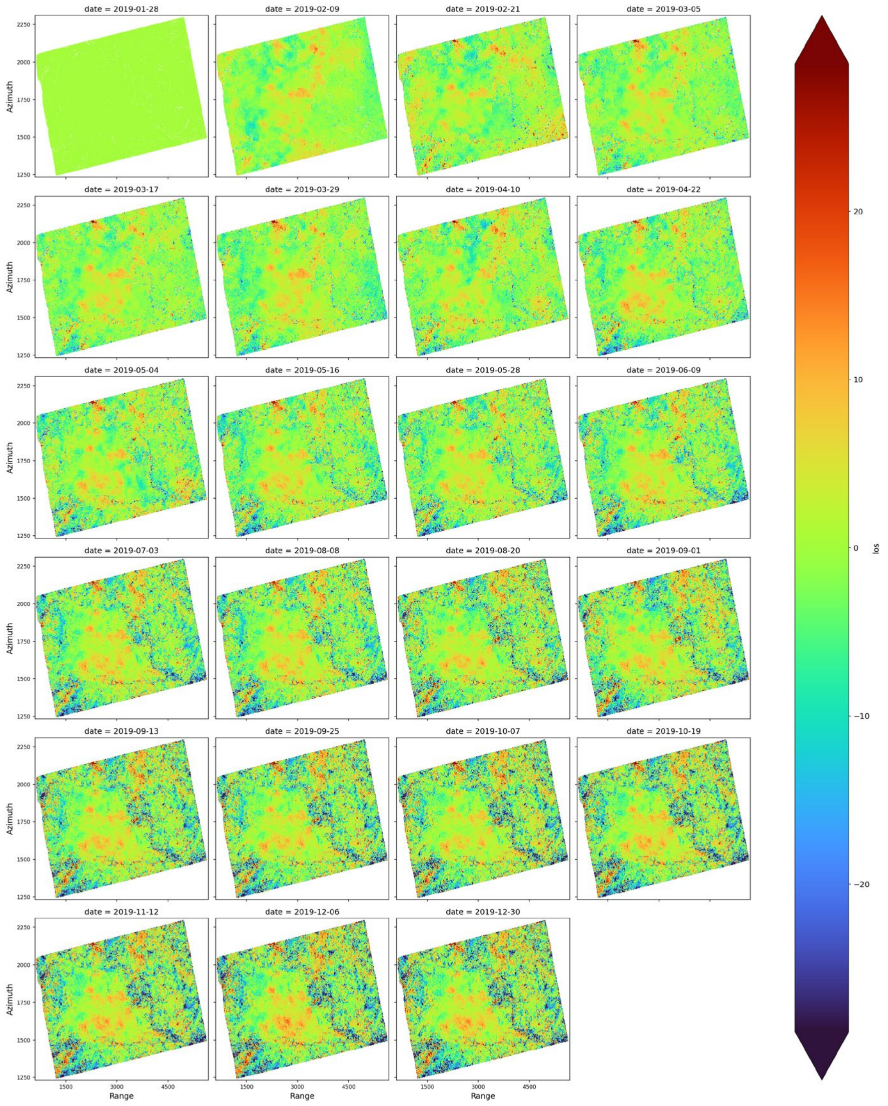

cumulative Line Of Sight displacement

The second component, **ground dynamic(03)**, focuses on ground deformation metrics, which include **"Phase", "Coherence" and "Amplitude"** Our dataset is also collected every 12 and 24 days and shares the same spatial resolution of 1008x969 pixels.

HIERARCHICAL TRANSFORMER FOR UNSUPERVISED LEARNING

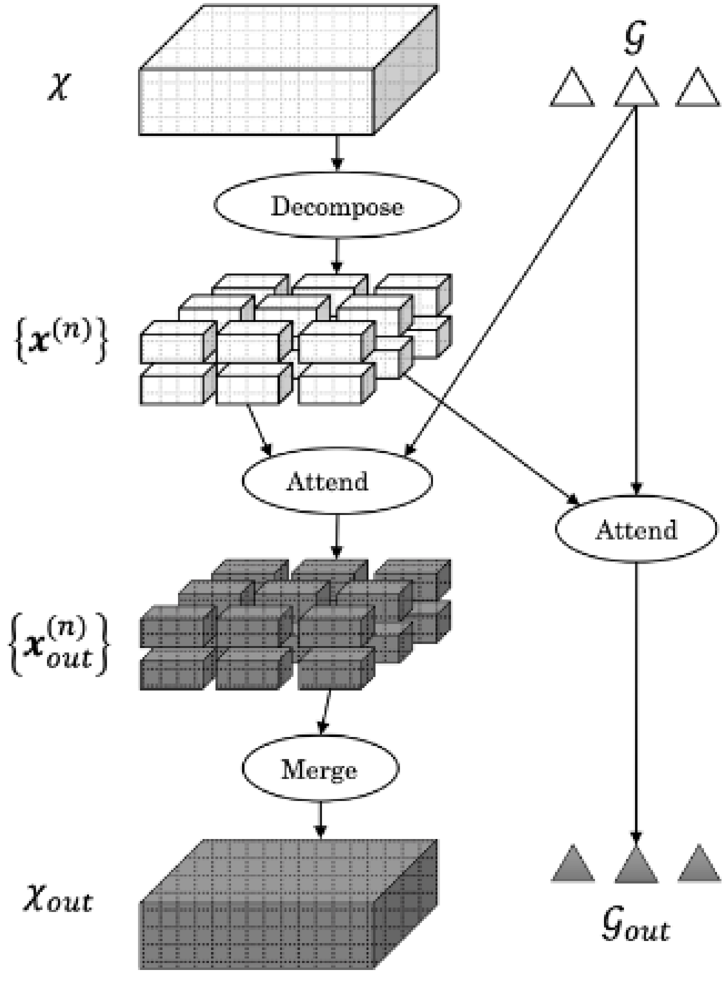

2) Cuboid attention with global vectors

X: Contextual Factors(07) + Ground dynamic(03)

$X^{(n)}$: spacetime decomposition + Attention.
N Days decomposition and 48x51 spatial resolution

$X^{(n)}_{out}$: Generation.
N Days rich learned representations

X_{out}, G_{out}: Merge.
capture complex relationships and dependencies

unsupervised learning techniques using **transformer architectures**, which utilize attention mechanisms **to capture complex relationships and dependencies across the dataset**. This approach enables the model to **generate rich "learned representations"** that take into account not only the contextual factors(07) but also the dynamic interactions observed in the ground deformation data(03).

Gao, Z., Shi, X., Wang, H., Zhu, Y., Wang, Y.B., Li, M., Yeung, D.Y.: Earthformer: Exploring space-time transformers for earth system forecasting. Advances in Neural Information Processing Systems 35 , 25390-25403 (2022)

transformer architectures

$$\mathcal{X}_{\text{out}}, \mathcal{G}_{\text{out}} = \text{CubAttn}_{\Theta}(\mathcal{X}, \mathcal{G}, \text{cuboid\_size}, \text{strategy}, \text{shift})$$

$$\Downarrow$$

$$\begin{aligned}
\{\boxed{x^{(n)}}\} &= \text{Decompose}(\mathcal{X}, \text{cuboid_size}, \text{strategy}, \text{shift}) \\
x^{(n)}_{\text{out}} &= \text{Attention}_{\Theta}(x^{(n)}, \text{Cat}(x^{(n)}, \mathcal{G}), \text{Cat}(x^{(n)}, \mathcal{G})) \\
\mathcal{G}_{\text{out}} &= \text{Attention}_{\Phi}(\mathcal{G}, \text{Cat}(\mathcal{G}, x^{(n)}), \text{Cat}(\mathcal{G}, x^{(n)})) \\
\mathcal{X}_{\text{out}} &= \text{Merge}\left(\left\{x^{(n)}_{\text{out}}\right\}_n, \text{cuboid_size}, \text{strategy}, \text{shift}\right)
\end{aligned}$$

Natural Breakpoint Method and supervised classification

We have chosen to **apply** the **natural breakpoint method** in order to **generate classes from our rich learned representations data**, in **response to the scarcity of available labels**.

Chen, L., Wang, W., Wu, W.B.: Inference of breakpoints in high-dimensional time series. Journal of the American Statistical Association 117 (540), 1951_x0015_1963 (2022)

Hurtado, S.I., Zaninelli, P.G., Agosta, E.A.: A multi-breakpoint methodology todetect changes in climatic time series. an application to wet season precipitationin subtropical argentina. Atmospheric Research 241 , 104955 (2020)

Topál, D., Matyasovszkyt, I., Kern, Z., Hatvani, I.G.: Detecting breakpoints inarti_x001C_cially modi_x001C_ed-and real-life time series using three state-of-the-art methods.Open geosciences 8 (1), 78_x0015_98 (2016)

Landlide Susceptibility Classes
Very Low (VL)
Low(L)
Moderate(M)
High(H)
Very High(VH)

Landslide Dynamic Susceptibility Mapping

Comparative Assessment of

RF

Yu, C.; Chen, J. Application of a GIS-Based Slope Unit Method for Landslide Susceptibility Mapping in Helong City: Comparative Assessment of ICM, AHP, and RF Model. Symmetry 2020, 12, 1848.

SVM

Vapnik, V. Support-vector networks. Mach. Learn. 1995, 20, 273–297.

CNN

LeCun, Y.; Bengio, Y. Convolutional networks for images, speech, and time series. In The Handbook of Brain Theory and NeuralNetworks; MIT Press: Boston, MA, USA, 1995; Volume 3361, pp. 255–258.

THANK!

Kemche Ghomsi Adrien Arnaud, Mvogo Ngono Joseph, Bowong Tsakou Samuel, Noumsi Woguia Auguste Vigny
UNIVERSITY OF DOUALA, Cameroon
adrien.ghomsi@weloobe.com